Shift in the absorption edge due to exchange interaction in ferromagnetic semiconductors

Shift in the absorption edge due to exchange interaction in ferromagnetic semiconductors

N Lebedeva[1] and P Kuivalainen[1,2]

[1] Helsinki University of Technology, Department of Electrical and Communication Engineering, Electron Physics Laboratory, PO Box 3000, FIN-02015 HUT, Finland
[2] VTT Information Technology, PO Box 1101 VTT, Finland

E-mail: pekka.kuivalainen@hut.fi

Abstract
We develop the theory of the shift in the band edge caused by a strong exchange interaction between charge carrier spins and the spins of the localized magnetic electrons in ferromagnetic semiconductors. The one-particle Green function is derived by using Matsubara's temperature Green functions, and then an infinite-order correction to the band edge due to the exchange interaction is determined from the poles of the Green function. With the aid of the temperature- and magnetic field-dependent spin polarization of the magnetic moments and the spin correlation functions, the band edge can be calculated as a function of temperature in various magnetic fields. The calculated results are compared to experimental data in the cases of the ferromagnetic semiconductors EuO and $Ga_{1-x}Mn_xAs$ over a wide temperature range. For these materials the values 0.223 and 1.4 eV are evaluated for the exchange interaction parameter, respectively. A new feature is found in the ferromagnetic region, as a result of the exceptionally strong exchange interaction in $Ga_{1-x}Mn_xAs$, i.e., a blue-shift in the band edge with decreasing temperature or with increasing magnetic field.

1. Introduction

During the last few decades, magnetic semiconductors such as Eu chalcogenides (EuO, EuS, EuSe, and EuTe) and spinels of the type $CdCr_2Se_4$ have been a focus of intensive scientific research. The unusual electrical, optical, and magnetic properties of these 'first-generation' magnetic semiconductors had already been investigated thoroughly in the

1970s [1]. Later, due to difficulties in fabricating these materials, the interest was focused more on diluted magnetic semiconductors (DMSs) such as $Cd_{1-x}Mn_xTe$ and $Zn_{1-x}Mn_xTe$, where the magnetic properties could be controlled by altering the magnetic Mn-ion content [2]. The DMSs could be called magnetic semiconductors of 'the second generation'.

The reason for the wide interest in the above-mentioned materials is that the magnetic semiconductors bridge between the physics of magnetism and the physics of semiconductors. One of the most attractive features found in these materials is a strong exchange interaction between the itinerant charge carriers and the localized magnetic moments. This interaction is manifested, e.g., as strong temperature and magnetic field dependences of the optical and electrical properties of the magnetic semiconductors. For instance, the ferromagnetic semiconductors display a strong red-shift in the fundamental optical absorption edge below the Curie temperature T_C or in high magnetic fields [1]. Also, in the resistivity a prominent peak at T_C has been found, which then disappears in sufficiently high magnetic fields, showing a large negative magnetoresistance.

Heavily Mn-doped GaAs is a recently found ferromagnetic semiconductor having a rather high T_C (up to 110 K) [3, 4]. We could call (Ga, Mn)As and related ferromagnetic materials magnetic semiconductors of 'the third generation'. A new feature of (Ga, Mn)As is the compatibility with conventional GaAs-based heterostructure technologies, which offers a new opportunity to study the optical and electrical properties of the ferromagnetic semiconductors in well-defined semiconductor devices having well-known band structures. The resistivity peak and the band splitting due to the exchange interaction have been observed experimentally in (Ga, Mn)As [4, 5]. However, there are several open questions related to the origin of magnetism and to the strength of the exchange interaction in (Ga, Mn)As. For instance, the experimental values for the exchange interaction parameter vary between 0.6 and 3.3 eV [4–7].

The theory of the shift in the optical absorption edge due to the exchange interaction in ferromagnetic semiconductors was developed first by Haas [8] and Rys *et al* [9]. Haas's result, which was based on the ordinary second-order perturbation theory, turned out to be divergent at T_C. Rys *et al* [9] applied an infinite-order perturbation theory, and their result was non-divergent, but valid only in a narrow temperature range above T_C in the cases where the average spin polarization of the magnetic atoms vanishes. The temperature and magnetic field dependences of the optical absorption edge predicted by these two models were never compared to experimental data.

In the present paper we develop further the theory of the shift in the band edge caused by the exchange interaction in ferromagnetic semiconductors by using Matsubara's temperature Green functions. We generalize the treatment presented previously by Rys *et al* [9] to the cases of non-zero average spin polarization, i.e., to the ferromagnetic temperature region and to the cases of non-zero applied magnetic fields. This allows us to verify the model by comparing the model predictions to the measured temperature and magnetic field dependences of the band edge over the whole temperature range including both paramagnetic and ferromagnetic regions. First we compare the calculated results to experimental data in the case of the 'standard' ferromagnetic semiconductor EuO. Then we apply the theory to the new ferromagnetic semiconductor (Ga, Mn)As in order to estimate, e.g., the value of the exchange parameter.

2. One-particle Green function

The dependence of the band edges on the magnetic order in the ferromagnetic semiconductors can be estimated by using the first- and second-order perturbation theory, as shown by Haas [8]. However, since the second-order correction of the band edge depends on the spin correlation functions, which diverge at $T = T_C$, the result is not valid at temperatures close to the magnetic ordering temperature. Therefore we have to apply an infinite-order perturbation theory based on Green functions [10]. In the case of (Ga, Mn)As the application of the second-order perturbation theory would be questionable also due to the fact that the exchange interaction between the itinerant holes and the localized magnetic moments is exceptionally large.

Let us consider a model ferromagnetic semiconductor, where free charge carriers move in an isotropic conduction or valence band described by a single effective mass m^*. Furthermore, we assume that the charge carrier spins interact strongly with the localized spins of the magnetic atoms through the exchange interaction. The total Hamiltonian describing the free carrier and magnetic subsystems as well as their mutual interaction is then given by

$$H_{tot} = H_c^0 + H_{exch} + H_m \tag{1}$$

where

$$H_c^0 = \frac{\vec{p}^2}{2m^*} \tag{2}$$

$$H_{exch} = -\Omega \sum_{\vec{R}} J(\vec{r} - \vec{R}) \vec{s} \cdot \vec{S}_{\vec{R}} \tag{3}$$

$$H_m = -\sum_{\vec{R},\vec{R}'} I(\vec{R}, \vec{R}') \vec{S}_{\vec{R}} \cdot \vec{S}_{\vec{R}'} - g_L \mu_B B \sum_{\vec{R}} S_{\vec{R}}^z. \tag{4}$$

H_c^0 gives the free carrier energies in the unperturbed band. The operator H_{exch} describes the exchange interaction between the free carrier spin $\vec{s}$ and the magnetic atom at a lattice point $\vec{R}$ having the total spin $\vec{S}_{\vec{R}}$. $\Omega = a_0^3/4$ is the volume of the unit cell in a FCC crystal lattice having a lattice constant a_0, and $J(\vec{r} - \vec{R})$ is the exchange integral. Here we assume that the exchange potential is rapidly varying over the unit cell, i.e., is a δ-like function, $J(\vec{r} - \vec{R}) = J_{exch} \delta(\vec{r} - \vec{R})$. The operator H_m is a Heisenberg Hamiltonian for the magnetic subsystem, $I(\vec{R}, \vec{R}')$ being the constant of magnetic coupling between the localized spins $S_{\vec{R}}$. The last term in (4) gives the Zeeman energy when an external magnetic field B has been applied.

Now we can calculate the energy spectrum of the perturbed band states from a retarded Green function for charge carriers [10], which is obtainable from Dyson's equation in momentum space:

$$G = \frac{G^0}{1 - G^0 \Sigma}. \tag{5}$$

Here G_0 and G are the free and perturbed Green functions, respectively, and Σ is the sum of all the irreducible self-energy parts obtained in an S-matrix expansion. The Hamiltonian (3) is treated as the perturbation. In order to utilize the Green function technique we have to express the total Hamiltonian (1) in the second-quantization form

$$\hat{H}_{tot} = \sum_{\sigma} \int \psi_\sigma^\dagger(\vec{r}) H_{tot} \psi_\sigma(\vec{r}) \, d^3\vec{r} = \sum_{\vec{k}\sigma} E_{\vec{k}\sigma}^0 a_{\vec{k}\sigma}^\dagger a_{\vec{k}\sigma} - \frac{\Omega}{2} \sum_{\vec{R}} \int J(\vec{r} - \vec{R}) \big\{ S_{\vec{R}}^+ \psi_\downarrow^\dagger(\vec{r}) \psi_\uparrow(\vec{r})$$

$$+ S_{\vec{R}}^- \psi_\uparrow^\dagger(\vec{r}) \psi_\downarrow(\vec{r}) + (S_{\vec{R}}^z - \langle S^z \rangle)[\Psi_\uparrow^\dagger(\vec{r}) \Psi_\uparrow(\vec{r}) - \Psi_\downarrow^\dagger(\vec{r}) \Psi_\downarrow(\vec{r})] \big\} \, d^3\vec{r} + H_m \tag{6}$$

where

$$\psi_\sigma^\dagger(\vec{r}) = \frac{1}{\sqrt{V}} \sum_{\vec{k}} a_{\vec{k}\sigma}^\dagger e^{-i\vec{k}\cdot\vec{r}} |\sigma\rangle \qquad \psi_\sigma(\vec{r}) = \frac{1}{\sqrt{V}} \sum_{\vec{k}} a_{\vec{k}\sigma} e^{i\vec{k}\cdot\vec{r}} |\sigma\rangle \tag{7}$$

are the charge carrier field operators, $a_{\vec{k}\sigma}^\dagger$ and $a_{\vec{k}\sigma}$ being the creation and annihilation operators, respectively, for a band state $|\vec{k}\sigma\rangle$ and $\sigma = (\uparrow, \downarrow)$ is the spin index. Here a plane wave representation normalized to the volume V is used for the band states $|\vec{k}\sigma\rangle = V^{-1/2} \exp(i\vec{k} \cdot \vec{r})|\sigma\rangle$. The spin raising and lowering operators are defined as usual by $S_{\vec{R}}^+ = S_{\vec{R}}^x + iS_{\vec{R}}^y$ and $S_{\vec{R}}^- = S_{\vec{R}}^x - iS_{\vec{R}}^y$, respectively.

The identity $S_{\vec{R}}^z = S_{\vec{R}}^z - \langle S^z \rangle + \langle S^z \rangle$ was inserted in (6), which allows us to redefine the spin polarized band energies as

$$E_{\vec{k}\sigma}^0 = \frac{\hbar^2 \vec{k}^2}{2m^*} - \frac{x}{2} J_{exch} \langle S^z \rangle (\delta_{\sigma\uparrow} - \delta_{\sigma\downarrow}) \tag{8}$$

where x is a mole fraction of the magnetic atoms, and $\langle S^z \rangle$ is the average spin polarization of the magnetic subsystem. The equation (8) already gives the first-order correction to the band energies. However, this correction is finite only for non-zero average spin polarization, i.e., when $T < T_C$ or when the external magnetic field has been applied. In order to describe the band shift at higher temperatures we have to take into account the higher-order corrections.

In the temperature interaction representation [10] the exchange part of the total Hamiltonian (6) is given by

$$\hat{H}_{exch}(\tau) = -\frac{\Omega}{2} \sum_{\vec{R}} \int J(\vec{r} - \vec{R})\{S_{\vec{R}}^+ \Psi_{\downarrow}^{\dagger}(\vec{r}, \tau)\Psi_{\uparrow}(\vec{r}, \tau) + S_{\vec{R}}^- \Psi_{\uparrow}^{\dagger}(\vec{r}, \tau)\Psi_{\downarrow}(\vec{r}, \tau)$$

$$+ (S_{\vec{R}}^z - \langle S^z \rangle)[\Psi_{\uparrow}^{\dagger}(\vec{r}, \tau)\Psi_{\uparrow}(\vec{r}, \tau) - \Psi_{\downarrow}^{\dagger}(\vec{r}, \tau)\Psi_{\downarrow}(\vec{r}, \tau)]\} \, d^3\vec{r} \tag{9}$$

where the field operators in the interaction picture read

$$\Psi_{\sigma}^{\dagger}(\vec{r}, \tau) = e^{\hat{H}_0\tau/\hbar}\psi_{\sigma}^{\dagger}(\vec{r})e^{-\hat{H}_0\tau/\hbar} \qquad \Psi_{\sigma}(\vec{r}, \tau) = e^{\hat{H}_0\tau/\hbar}\psi_{\sigma}(\vec{r})e^{-\hat{H}_0\tau/\hbar}. \tag{10}$$

Here $\hat{H}_0$ is the Hamiltonian of the system without the exchange interaction (9).

Matsubara's temperature Green function is defined as

$$G_{\sigma\sigma'}(\vec{r}, \tau; \vec{r}', \tau') = -\langle T_{\tau}\hat{S}\Psi_{\sigma}(\vec{r}, \tau)\Psi_{\sigma'}^{\dagger}(\vec{r}', \tau')\rangle_{con} \tag{11}$$

where the brackets $\langle \cdots \rangle_{con}$ denote the thermal average, and we retain only terms corresponding to connected diagrams in the series expansion. T_{τ} is a time ordering operator, and the S-matrix is defined as

$$\hat{S} = \exp\left[-\int_0^{\beta\hbar} \hat{H}_{exch}(\tau) \, d\tau/\hbar\right] \tag{12}$$

where $\beta = 1/k_B T$. The unperturbed Green function is given by [10]

$$G_{\sigma\sigma'}^0(\vec{r}, \tau; \vec{r}', \tau') = -\langle T_{\tau}\Psi_{\sigma}(\vec{r}, \tau)\Psi_{\sigma'}^{\dagger}(\vec{r}', \tau')\rangle = \frac{1}{\hbar V \beta} \sum_{n\vec{k}} e^{i\vec{k}\cdot(\vec{r}-\vec{r}')-i\omega_n(\tau-\tau')} G_{\sigma\sigma'}^0(\vec{k}, \omega_n)$$

$$= \frac{\delta_{\sigma\sigma'}}{\hbar V \beta} \sum_{n\vec{k}} \frac{e^{i\vec{k}\cdot(\vec{r}-\vec{r}')-i\omega_n(\tau-\tau')}}{i\omega_n - E_{\vec{k}\sigma}^0/\hbar} \tag{13}$$

where $\omega_n = (2n+1)\pi/\hbar\beta$ (n is an integer), and $G_{\sigma\sigma'}^0(\vec{k}, \omega_n)$ is the Fourier transform of $G_{\sigma\sigma'}^0(\vec{r}, \tau; \vec{r}', \tau')$.

Next we determine the perturbed Green function from (5), and therefore we need an approximation for the self-energy. The second-order self-energy is obtainable from the second-order correction in the expansion (11). Inserting the S-matrix (12) into the Green function (11), and taking into account only the terms proportional to J_{exch}^2, we get the following second-order Green function:

$$G_{\sigma\sigma'}^{(2)}(\vec{r}, \tau; \vec{r}', \tau') = -\left\langle T_{\tau} \frac{1}{2\hbar^2} \int_0^{\beta\hbar} d\tau_1 \int_0^{\beta\hbar} \hat{H}_{exch}(\tau_1)\hat{H}_{exch}(\tau_2)\Psi_{\sigma}(\vec{r}, \tau)\Psi_{\sigma'}^{\dagger}(\vec{r}', \tau') \, d\tau_2 \right\rangle_{con}. \tag{14}$$

The relevant thermal average in (14) can be estimated by using the Hamiltonian (9) and retaining only the terms linear in the spin correlation function $\propto \langle \vec{S}_{\vec{R}} \cdot \vec{S}_{\vec{R}'} \rangle$. Using the definition of the zero-order Green function (13), we can write the terms appearing in (14) in a compact form:

$$\langle T_\tau \hat{H}_{exch}(\tau_1) \hat{H}_{exch}(\tau_2) \Psi_\sigma(\vec{r}, \tau) \Psi_{\sigma'}^\dagger(\vec{r}', \tau') \rangle_{con}$$

$$= \frac{\Omega^2}{2} \sum_{\vec{R}, \vec{R}'} \int d^3x \int d^3x' \, J(\vec{x} - \vec{R}) J(\vec{x}' - \vec{R}') \{ \Gamma^{xx}(\vec{R}, \vec{R}')$$

$$\times G_{\uparrow\sigma}^0(\vec{x}, \tau_1; \vec{r}, \tau) G_{\downarrow\downarrow}^0(\vec{x}, \tau_1; \vec{x}', \tau_2) G_{\uparrow\sigma'}^0(\vec{x}', \tau_2; \vec{r}', \tau')$$

$$+ \Gamma^{yy}(\vec{R}, \vec{R}') G_{\downarrow\sigma}^0(\vec{x}, \tau_1; \vec{r}, \tau) G_{\uparrow\uparrow}^0(\vec{x}, \tau_1; \vec{x}', \tau_2) G_{\downarrow\sigma'}^0(\vec{x}', \tau_2; \vec{r}', \tau')$$

$$+ \Gamma^{zz}(\vec{R}, \vec{R}') G_{\sigma\sigma'}^0(\vec{x}, \tau_1; \vec{r}, \tau) G_{\sigma\sigma'}^0(\vec{x}, \tau_1; \vec{x}', \tau_2) G_{\sigma\sigma'}^0(\vec{x}', \tau_2; \vec{r}', \tau') \} \tag{15}$$

where the spin correlation functions are defined as $\Gamma(\vec{R}, \vec{R}') = \langle (\vec{S}_{\vec{R}} - \langle \vec{S}_{\vec{R}} \rangle) \cdot (\vec{S}_{\vec{R}'} - \langle \vec{S}_{\vec{R}'} \rangle) \rangle$. Using the familiar sum rule $\sum \exp[i(\vec{k} - \vec{p}) \cdot \vec{R}] = \delta_{\vec{k}, \vec{p}} N$ over the lattice sites $\vec{R}$, and inserting (15) into (14), we obtain the second-order Green function in the momentum space as follows:

$$G_{\sigma\sigma'}^{(2)}(\vec{k}, \omega_n) = G_{\uparrow\sigma'}^0(\vec{k}, \omega_n) \left[\frac{J_{exch}^2}{4N} \sum_{\vec{q}} \frac{\Gamma^{xx}(\vec{q}) \delta_{\uparrow\sigma'}}{i\hbar\omega_n - E_{\vec{k}-\vec{q},\downarrow}^0} \right] G_{\uparrow\sigma'}^0(\vec{k}, \omega_n)$$

$$+ G_{\downarrow\sigma'}^0(\vec{k}, \omega_n) \left[\frac{J_{exch}^2}{4N} \sum_{\vec{q}} \frac{\Gamma^{yy}(\vec{q}) \delta_{\downarrow\sigma'}}{i\hbar\omega_n - E_{\vec{k}-\vec{q},\uparrow}^0} \right] G_{\downarrow\sigma'}^0(\vec{k}, \omega_n)$$

$$+ G_{\sigma\sigma'}^0(\vec{k}, \omega_n) \left[\frac{J_{exch}^2}{4N} \sum_{\vec{q}} \frac{\Gamma^{zz}(\vec{q}) \delta_{\sigma\sigma'}}{i\hbar\omega_n - E_{\vec{k}-\vec{q},\sigma}^0} \right] G_{\sigma\sigma'}^0(\vec{k}, \omega_n) \tag{16}$$

where $\Gamma(\vec{q})$ is the Fourier transform of the spin correlation function.

Now we can identify the second-order self-energy from (16):

$$\Sigma_{\sigma\sigma'}^{(2)}(\vec{k}, \omega_n) = \frac{J_{exch}^2}{4N} \delta_{\sigma\sigma'} \sum_{\vec{q}} \left[\frac{\Gamma^{xx}(\vec{q}) \delta_{\sigma\uparrow}}{i\hbar\omega_n - E_{\vec{k}-\vec{q},\downarrow}^0} + \frac{\Gamma^{yy}(\vec{q}) \delta_{\downarrow\sigma'}}{i\hbar\omega_n - E_{\vec{k}-\vec{q},\uparrow}^0} + \frac{\Gamma^{zz}(\vec{q}) \delta_{\sigma\sigma'}}{i\hbar\omega_n - E_{\vec{k}-\vec{q},\sigma}^0} \right]. \tag{17}$$

The first two terms in (17) are related to spin-flip transitions due the exchange interaction (9), whereas the last term describes the interaction without spin-flip processes. By using the Dyson equation (5), we can finally solve the perturbed Green function, which reads

$$G_{\sigma\sigma'}(\vec{k}, \omega_n) = \frac{\hbar \delta_{\sigma\sigma'}}{i\hbar\omega_n - E_{\vec{k}\sigma}^0 - \Sigma_{\sigma\sigma'}^{(2)}(\vec{k}, \omega_n)}. \tag{18}$$

The poles of the real part of the denominator in (18) give the perturbed band energy:

$$E_{\vec{k}\sigma} = E_{\vec{k}\sigma}^0 + \frac{J_{exch}^2}{4N'} \sum_{\vec{q}} \left[\frac{\Gamma^{xx}(\vec{q}) \delta_{\sigma\uparrow}}{E_{\vec{k}\sigma} - E_{\vec{k}-\vec{q},\downarrow}^0} + \frac{\Gamma^{yy}(\vec{q}) \delta_{\downarrow\sigma'}}{E_{\vec{k}\sigma} - E_{\vec{k}-\vec{q},\uparrow}^0} + \frac{\Gamma^{zz}(\vec{q})}{E_{\vec{k}\sigma} - E_{\vec{k}-\vec{q},\sigma}^0} \right]. \tag{19}$$

Notice that the first-order correction is included in (19) through the equation (8). Haas [8] has obtained an energy correction similar to (19) by using the ordinary second-order perturbation theory. However, since only the first-order corrections (8) appeared in the denominator of the J_{exch}^2-term, Haas's result turned out to be divergent at T_C due to the divergence of the spin correlation functions (see below). Our result (19) shows the advantage of the infinite-order perturbation theory based on the Green function technique: the perturbed band energy $E_{\vec{k}\sigma}$ to be calculated appears in the denominator of the J_{exch}^2-term in (19), which removes the divergence at T_C. When the net spin polarization of the magnetic subsystem vanishes, $\langle S^z \rangle = 0$, equation (19) reduces to the result derived previously by Rys *et al* [9]. However, their result is valid only in the paramagnetic region, i.e., when $\langle S^z \rangle = 0$, whereas our result (19) is valid over the whole temperature range and also in the case of non-zero magnetic fields.

3. Calculation of the band shift

In order to calculate the changes of the band edge as a function of temperature and applied magnetic field from (19), we have to know the wavevector dependence of the spin correlation functions $\Gamma(\vec{q}) = \Gamma^{xx}(\vec{q}) + \Gamma^{yy}(\vec{q}) + \Gamma^{zz}(\vec{q})$. Expressions for these functions can be derived, e.g., by applying the procedure proposed by Sinkkonen [11].

In the molecular field approximation (MFA) the average spin polarization of the magnetic moments is given by

$$N^{-1}\sum_{\vec{R}} \langle S_{\vec{R}}^z \rangle = x\langle S^z \rangle = xSB_S(y) = x\left(\frac{2S+1}{2}\right)\coth\left(\frac{2S+1}{2S}y\right) - \frac{x}{2}\coth\left(\frac{y}{2S}\right) \tag{20}$$

where $B_S(y)$ is the Brillouin function with

$$y = \frac{g_L\mu_B S}{k_B T}B_{eff} \tag{21}$$

and the effective molecular field acting on the spin $\vec{S}_{\vec{R}}$ is obtained from the magnetic Hamiltonian (4):

$$B_{eff} = B + \frac{2I(\vec{q}=0)\langle S^z \rangle}{g_L\mu_B}. \tag{22}$$

$I(\vec{q})$ is the Fourier transform of the magnetic coupling parameter $I(\vec{R}, \vec{R}')$ in (4), and in the case of the FCC lattice it is given by [12]

$$I(\vec{q}) = \frac{3k_B T_C}{2S(S+1)}\left[1 - \frac{a_0^2 q^2}{12}\right]. \tag{23}$$

When calculating the spin correlation functions in the case of DMSs by using the method of [11], we have to take into account that a magnetic moment is found at a lattice site $\vec{R}$ with a probability x (as in the lattice summation in (20)). Then we have

$$\Gamma^{xx}(\vec{q}) = \Gamma^{yy}(\vec{q}) = \frac{xS^2 B_S(y)/y}{1 - \frac{2S^2 I(\vec{q})B_S(y)/y}{k_B T}}$$

$$\Gamma^{zz}(\vec{q}) = \frac{xS^2\,\partial B_S(y)/\partial y}{1 - \frac{2S^2 I(\vec{q})\,\partial B_S(y)/\partial y}{k_B T}}. \tag{24}$$

The temperature dependence of the spin correlation functions (24) shows a divergence at T_C, $\Gamma \propto (T - T_C)^{-1}$. This behaviour is shown in figure 1, where $\Gamma^{zz}(\vec{q}=0)$ is plotted as a function of temperature in various magnetic fields. The material parameters were those of EuO (see below).

By using the wavevector-dependent spin correlation functions (24) and the magnetic coupling parameter (23), we can integrate in a closed form over the wavevector q in (19). Assuming a parabolic band we get the following expression for the band edge $E_\uparrow(\vec{k}=0)$ in the case of the spin-up charge carriers:

$$E_\uparrow(\vec{k}=0) = -\frac{\Delta}{2} - \frac{xJ_{exch}^2\Omega m*}{8\hbar^2\pi}[F_1(E_\uparrow(\vec{k}=0)) + F_2(E_\uparrow(\vec{k}=0))] \tag{25}$$

where

$$F_1(E_\uparrow(\vec{k}=0)) = \frac{A}{c}\left[\sqrt{\frac{b}{c}} + \sqrt{\frac{2m*}{\hbar^2}\,\mathrm{Re}\left\{|E_\uparrow(\vec{k}=0)| + \frac{\Delta}{2}\right\}}\right]^{-1} \tag{26}$$

$$F_2(E_\uparrow(\vec{k}=0)) = \frac{D}{f}\left[\sqrt{\frac{e}{f}} + \sqrt{\frac{2m*}{\hbar^2}\left\{|E_\uparrow(\vec{k}=0)| - \frac{\Delta}{2}\right\}}\right]^{-1} \tag{27}$$
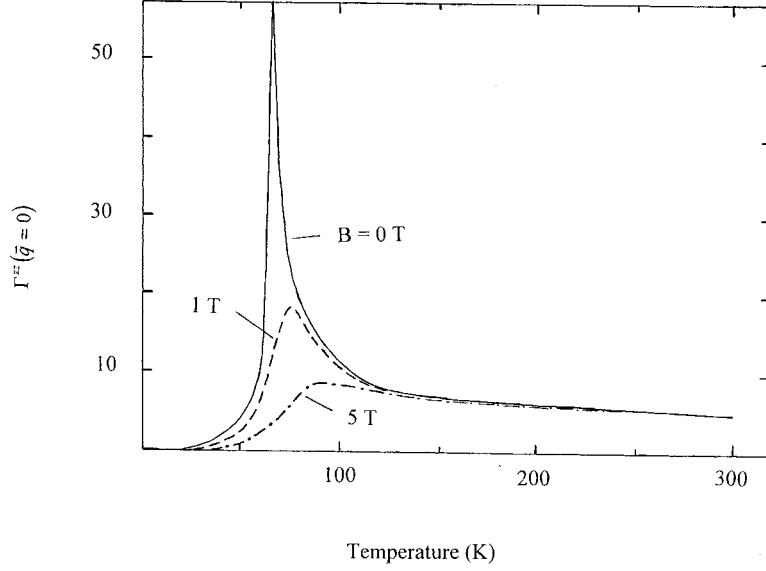
Figure 1. Spin correlation function $\Gamma^{zz}(\vec{q} = 0)$ versus temperature in various magnetic fields in EuO.

with $A = S^2 B_S(y)/y$, $D = S^2 \, \partial B_S(y)/\partial y$, and $\Delta = x J_{exch} \langle S^z(T, B) \rangle \rangle$, and

$$b = 1 - \frac{2S^2 I(\vec{q} = 0) B_S(y)/y}{k_B T} \tag{28}$$

$$c = \frac{S^2 I(\vec{q} = 0) a_0^2 B_S(y)/y}{6 k_B T} \tag{29}$$

$$e = 1 - \frac{2S^2 I(\vec{q} = 0) \, \partial B_S(y)/\partial y}{k_B T} \tag{30}$$

$$f = \frac{S^2 I(\vec{q} = 0) a_0^2 \, \partial B_S(y)/\partial y}{6 k_B T}. \tag{31}$$

From (25) the band edge $E_\uparrow(\vec{k} = 0)$ can be solved self-consistently by using numerical iteration. An expression for the spin-down carriers can be derived simply by replacing Δ by $-\Delta$ in (25)–(27).

4. Numerical results for EuO and GaMnAs

In order to verify the theory of the band shift developed above we can apply it to the experimental data obtained in the case of the 'standard' ferromagnetic semiconductor EuO. In EuO the magnetic electrons occupy a well-localized 4f level and the charge carriers move in a broad s-type conduction band. When the magnetic ordering occurs, i.e., when $\langle S^z \rangle \neq 0$, the energy of the seven 4f electrons does not change, but the conduction electrons become spin polarized according to (8). Therefore the measured red-shift of the optical absorption edge below T_C or in applied magnetic fields is believed to be related directly to the shift of the conduction band edge for spin-up electrons in EuO [1].

Figure 2 shows the comparison of the results calculated from (25) to the measured [1] band shift at $B = 0$ and 1.35 T. The theoretical results agreed reasonably well with the measured
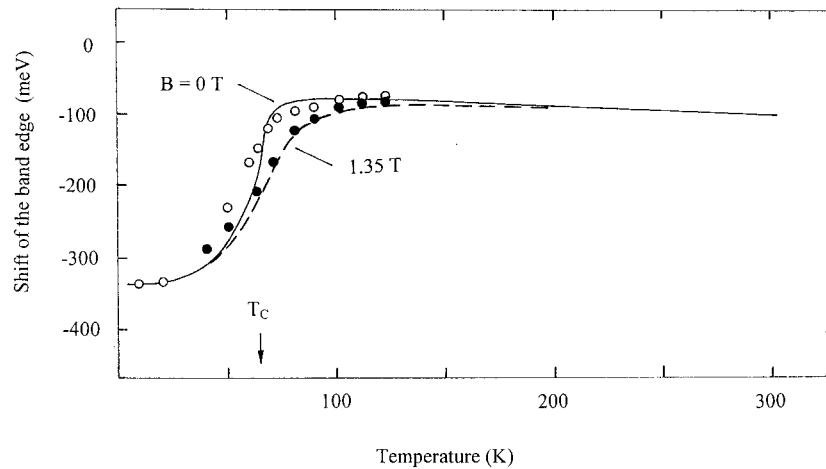
Figure 2. Calculated and measured band shift in EuO. The solid curve has been calculated from (25) at $B = 0$ T and the dashed curve at $B = 1.35$ T. The experimental data were taken from [1]: the white dots were measured at $B = 0$ T and the black dots at $B = 1.35$ T.

ones, when the following material parameters were used: $J_{exch} = 0.223$ eV, $T_C = 65$ K, $a_0 = 5.15$ Å, $S = 7/2$, and $m* = 1.0$ m_0. These values are almost the same as those mentioned for EuO in [1]. However, the exchange interaction parameter J_{exch} is slightly larger in our case than the value 0.18 eV estimated in [1]. This is probably due to the fact that we took into account the higher-order corrections in our expression (25), whereas the value mentioned in [1] was most probably estimated from the first-order result (8).

The higher-order corrections to the band edge in (25) give a non-zero contribution to the band edge ≈ 0.1 eV already in the paramagnetic region $T > T_C$, where the net spin polarization (and consequently the first-order result $\Delta/2$) vanishes at $B = 0$ T. In the calculated results of figure 2 there is a small blue-shift $\approx 10^{-4}$ eV K^{-1} as temperature decreases in the paramagnetic region $T \gg T_C$. This is of the same order of magnitude as the measured blue-shift in EuO [1]. Usually this behaviour is explained by a lattice dilatation and an electron–phonon interaction. However, our calculations show that there also may be a magnetic contribution related to the temperature dependence of the spin correlation functions shown in figure 1. At temperatures close to T_C the spin correlation functions increase strongly, as shown in figure 1. This behaviour together with a strong increase of the net magnetization at $T < T_C$ result in a large red-shift in the band edge near the magnetic ordering temperature. Also the red-shift is well described by our theory, as shown in figure 2. The significance of the higher-order terms in (25) is clearly shown at temperatures close to T_C in the paramagnetic region, where the large increase in the spin correlation functions (see figure 1) in the higher-order terms causes a strong red-shift already at temperatures where the average spin polarization and, thereby, the first-order band shift (8) vanish at $B = 0$ T. The application of the external magnetic field increases strongly the net magnetization at temperatures close to T_C. Consequently, the band edge shifts to lower energies, as shown both in the calculated and experimental results of figure 2.

In the recently found ferromagnetic semiconductor (Ga, Mn)As the exchange interaction parameter J_{exch} for electrons in the conduction band is of the same order of magnitude as the one in EuO [5, 13]. However, the exchange parameter for holes in the valence band seems to be an order of magnitude larger, $J_{exch} \approx 2$ eV. This large value emphasizes the higher-order corrections in (25), and therefore the temperature and magnetic field dependences of
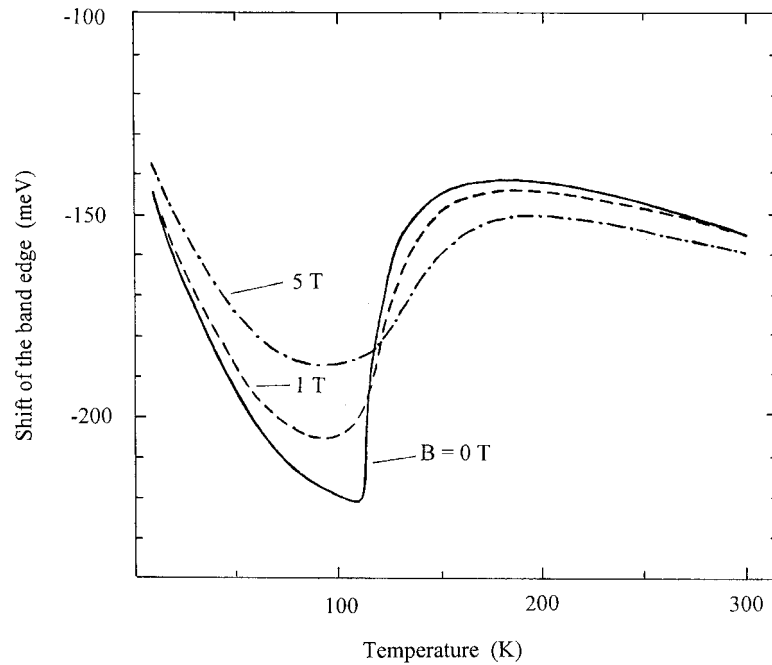
Figure 3. Calculated shift of the band edge for holes in the valence band of (Ga, Mn)As as a function of temperature in various magnetic fields.

the band edge may become dominated by the spin correlation functions and not by the net magnetization as in the case of EuO. In (Ga, Mn)As the itinerant charge carriers move in the well-characterized conduction and valence bands, and the magnetic electrons have been localized at the 3d level of the Mn atoms. Figure 3 shows the band edge for holes in the valence band of (Ga, Mn)As as a function of temperature in various magnetic fields. The band edge was calculated from (25) by using the following material parameters [4, 13]: $J_{exch} = 2.4$ eV, $m* = 0.5\ m_0$ (heavy holes), $a_0 = 5.65$ Å, $T_C = 110$ K, $S = 5/2$, and $x = 0.053$.

Figure 3 shows that in the paramagnetic region at temperatures close to the critical temperature there is a red-shift in energy with decreasing temperature or with increasing magnetic field, just as in the case of EuO. However, below T_C a blue-shift appears both with decreasing temperature and with increasing magnetic field. This is a new feature predicted by our model, which has not been found in the conventional magnetic semiconductors. The blue-shift is a result of the exceptionally large exchange interaction parameter, which emphasizes the higher-order corrections in (25): in the conventional ferromagnetic semiconductors such as EuO, the first-order result (8) dominates, and therefore the band shift is determined by the temperature and magnetic field dependences of the net magnetization. However, in the case of the large exchange interaction parameter the spin correlation functions in the higher-order terms of (19) (and (25)) start to dominate, and then the temperature and magnetic field dependences of the band edge are more related to those of the spin correlation functions. Figure 1 shows that below T_C the spin correlation functions decrease strongly with decreasing temperature and with increasing magnetic field. This explains the anomalous behaviour of the band edge in the ferromagnetic region in figure 3.

The blue-shift predicted by our model in figure 3 has not yet been studied experimentally in bulk (Ga, Mn)As. However, there are some experimental magnetoabsorption data on the
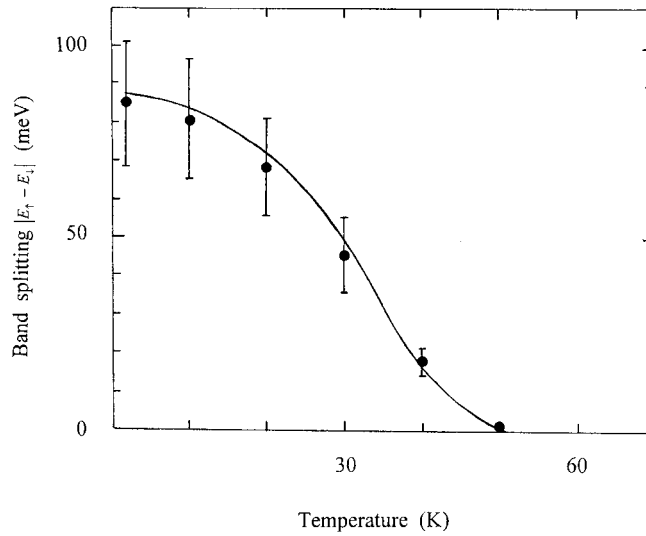
Figure 4. Experimental and calculated (solid curve) absorption edge splitting in (Ga, Mn)As versus temperature at $B = 0.02$ T. The experimental data were taken from [5].

ferromagnetic $Ga_{1-x}Mn_xAs$ epilayers [5]. Figure 4 shows the experimental and calculated absorption edge splitting versus temperature in $Ga_{1-x}Mn_xAs$ at $B = 0.02$ T. The theoretical result was calculated from (25) (and the same kind of equation for the spin-down carriers) by using the following material parameters [5]: $T_C = 39$ K and $x = 0.032$. The exchange parameter $J_{exch} = 1.4$ eV was used as a fitting parameter. This value is slightly smaller than the estimate 1.9–2.4 eV published by Szczytko *et al* [5], when they used the first-order result (8) only. This difference is partly explained by the fact that we neglected the band splitting of the conduction band, which should be taken into account when the absorption edge splitting is estimated. However, since the exchange parameter for the conduction electrons is an order of magnitude smaller than the one for holes, and since the experimental errors in figure 4 are large, the fitting of the calculated results to the experimental data of figure 4 would have been inaccurate even if the conduction band splitting had been included. Therefore the good fit shown in figure 4 cannot be considered any verification of the model, and more experimental data on magnetoabsorption in bulk (Ga, Mn)As close to T_C are needed in order to verify, e.g., the behaviour predicted by our model in figure 3.

5. Conclusions

The infinite-order perturbation theory for the exchange interaction between the itinerant carrier spins and the localized magnetic moments in the ferromagnetic semiconductors allows us to calculate the band shift both in the paramagnetic and ferromagnetic regions in various magnetic fields. The theory describes well the temperature and magnetic field dependences of the band shift in the conventional magnetic semiconductors such as EuO. Our results show the importance of the higher-order corrections to the band edge when extracting the exchange interaction parameter from the measured red-shift. Also the theory predicts that in the new ferromagnetic semiconductor (Ga, Mn)As the exceptionally large exchange interaction between the holes and the magnetic 3d electrons results in an anomalous blue-shift in the band edge in the ferromagnetic region. This blue-shift has not yet been measured in bulk (Ga, Mn)As,

and our present theoretical results should encourage experimentalists to study the band shift more carefully at temperatures close to the critical temperature.

References

[1] Wachter P 1972 *CRC Crit. Rev. Solid State Sci.* **3** 189
[2] Balkanski M and Averous M (ed) 1991 *Diluted Magnetic Semiconductors* (New York: Plenum)
[3] Ohno H, Shen A, Matsukura F, Oiwa A, Endo A, Katsumoto S and Iye Y 1996 *Appl. Phys. Lett.* **69** 363
[4] Matsukura F, Ohno H, Shen A and Sugawara Y 1998 *Phys. Rev.* B **57** R2037
[5] Szczytko J, Mac W, Twardowski A, Matsukura F and Ohno H 1999 *Phys. Rev.* B **59** 12 935
[6] Ohno H, Akiba N, Matsukura F, Shen A, Ohtani K and Ohno Y 1998 *Appl. Phys. Lett.* **33** 363
[7] Ohno H and Matsukura F 2001 *Solid State Commun.* **117** 179
[8] Haas C 1968 *Phys. Rev.* **168** 531
[9] Rys F, Helman J S and Baltensperger W 1967 *Phys. Kondens. Mater.* **6** 105
[10] Fetter A L and Walecka J D 1971 *Quantum Theory of Many-Particle Systems* (New York: McGraw-Hill)
[11] Sinkkonen J 1980 *Phys. Rev.* B **23** 6638
[12] Kaski K, Sinkkonen J, Kuivalainen P and Stubb T 1980 *J. Phys. C: Solid State Phys.* **13** 5233
[13] Szczytko J, Mac W, Stachov A, Twardowski A, Becla P and Tworzydlo 1996 *Solid State Commun.* **99** 927